

Copyright  
by  
Sarah Yvonne Greer  
2018

The Thesis committee for Sarah Yvonne Greer  
Certifies that this is the approved version of the following thesis:

**A data matching algorithm and its applications in seismic  
data analysis**

APPROVED BY

SUPERVISING COMMITTEE:

---

Dr. Sergey Fomel, Supervisor

---

Dr. Kyle Spikes

---

Dr. Clark Wilson

**A data matching algorithm and its applications in seismic  
data analysis**

**by**

**Sarah Yvonne Greer**

**THESIS**

Presented to the Faculty of  
The University of Texas at Austin  
in Partial Fulfillment  
of the Requirements  
for the Degree of

**BACHELOR OF SCIENCE**

THE UNIVERSITY OF TEXAS AT AUSTIN

May 2018

## Acknowledgments

Add acknowledgements here :)

# **A data matching algorithm and its applications in seismic data analysis**

Sarah Yvonne Greer, B.S.

The University of Texas at Austin, 2018

Supervisor: Dr. Sergey Fomel

Abstract

## Table of Contents

Acknowledgments	iv
Abstract	v
List of Tables	vii
List of Figures	viii
Chapter 1. Balancing local frequency content in seismic data using non-stationary smoothing	1
Bibliography	15
Vita	17

## List of Tables

## List of Figures

1.1	Initial legacy (a) and high-resolution (b) images. These images show the same subsurface geology, but look remarkably different as the high-resolution image has distinctly higher frequency content than the legacy image. . . . .	6
1.2	The smoothing radius, which is a function of time and space, this method produces after 5 iterations. This represents the number of samples in time that the high-resolution image needs to be smoothed over in a triangle weight to balance local frequency content with the legacy image. . . . .	7
1.3	Spectral content of the legacy (red) and high-resolution (blue) images before (a) and after (b) spectral balancing. . . . .	9
1.4	Difference in local frequencies (residual) between the legacy and high-resolution images before (a) and after (b) the 5th iteration of frequency balancing. . . . .	11
1.5	Initial PP (a) and SS (b) images. . . . .	13
1.6	Interleaved PP and warped SS traces before (a) and after (b) frequency balancing and residual registration. After registration, the signal content between the two initial images is more aligned; for example, the reflections around 0.3 and 0.6 s. This indicates a successful registration. . . . .	14



# Chapter 1

## Balancing local frequency content in seismic data using non-stationary smoothing

Seismic data can experience non-stationary frequency variations caused by attenuation. This problem is encountered when matching multiple data sets, such as in multicomponent image registration, because signals with differing frequency content are hard to correlate. In this paper, we propose a method to balance frequency content between data sets while taking into account non-stationary frequency variations. This method involves finding and applying a non-stationary smoothing operator to minimize the local frequency difference between data sets. Numerical examples demonstrate that the proposed method improves multicomponent image registration and matching images of differing resolution.

### INTRODUCTION

Matching seismic data has many applications in geophysical processing methods, such as multi-component image registration, time-lapse image registration, matching well-ties to seismic data, and merging seismic data sets (Ursenbach et al., 2013; Fomel and Backus, 2003; Lumley et al., 2003; Herrera and van der Baan, 2012). Typically, the workflow for matching data involves finding the optimal time shift, or amount of stretching and compressing, of one trace relative to the other that produces the greatest similarity between the two traces, as seen in dynamic time warping and local

similarity scanning (Hale, 2013; Fomel and Jin, 2009; Herrera et al., 2014). However, when the two signals that need to be aligned have different spectral content, their comparison can be difficult. Most seismic data experience non-stationary, or spatially and temporally variant, frequency content caused by attenuation. This problem was discussed in application to multicomponent image registration by Fomel and Backus (2003), who applied frequency balancing methods to improve registration results. Liu and Fomel (2012) proposed using local time-frequency decomposition (LTFD) to balance frequencies between multicomponent data during registration. However, LTFD is a relatively computationally expensive method.

In this paper, we propose a method to remove non-stationary frequency differences that limit the effectiveness of matching data. We suggest applying the proposed method to processing flows that involve matching data before attempting to find the time shift to align their signal content. To balance frequency content, we use a non-stationary smoothing operator with an adjustable smoothing radius to apply to the higher frequency data set. Our approach takes the form of an optimization problem which is solved using an iterative method. We apply this method to examples of merging high-resolution and conventional seismic images and multicomponent image registration.

## METHOD

Two signals of differing frequencies are more difficult to correlate than signals of similar frequencies. For example, Figure 1.1 shows two seismic images representing the same subsurface, except they have distinctly different spectral content, as shown in Figure 1.3(a). In order to be directly comparable, these two images should have similar frequency content. In this paper, we look at local frequency (Fomel, 2007),

which can be thought of as a smoothed estimate of instantaneous frequency (White, 1991). Local frequency is a more geologically accurate attribute than instantaneous frequency because it honors time-frequency uncertainty and does not contain physically unrealistic negative or extremely high frequency values (Fomel, 2007).

In order to balance local frequency content, we propose smoothing the higher frequency data using a non-stationary triangle smoothing operator with an adjustable radius. Here, the radius at each point is the number of samples in time that that specific data point gets averaged over in a triangle weight.

Our goal is to find the temporally and spatially variable smoothing radius,  $\mathbf{R}$ , that minimizes the difference in local frequencies between the two data sets. This can be shown in the objective function

$$\min_{\mathbf{R} \in [1, N]} \left\| \mathbf{F}[\mathbf{S}_{\mathbf{R}} \mathbf{d}_h] - \mathbf{F}[\mathbf{d}_l] \right\|, \quad (1.1)$$

where  $\mathbf{S}_{\mathbf{R}}$  is the non-stationary smoothing operator of smoothing radius  $\mathbf{R}$ ,  $\mathbf{d}_h$  is the higher frequency data,  $\mathbf{d}_l$  is the lower frequency data,  $\mathbf{F}$  is the local frequency operator, and  $N$  is the maximum size of the smoothing radius. Although smoothing is a linear operation, the smoothed data,  $\mathbf{S}_{\mathbf{R}} \mathbf{d}_h$ , depends non-linearly on  $R$ . However, the objective from equation (1.1) is nearly convex, and we choose to use an intuitive iterative approach to find an approximate smoothing radius.

The main premise behind the method comes from the fact that, in general, the greater the smoothing radius, the more high frequencies are attenuated by smoothing. We choose an initial guess of the non-stationary smoothing radius before applying corrections based on two primary assumptions:

1. The smoothing radius is too *small* at a specified point if, after smoothing, the

higher frequency data has *higher* local frequency than the lower frequency data.

Thus, the smoothing radius must be *increased* at that point.

2. The smoothing radius is too *large* at a specified point if, after smoothing, the higher frequency data has *lower* local frequency than the lower frequency data.

Thus, the smoothing radius must be *decreased* at that point.

We apply these assumptions using a line-search method:

$$\mathbf{R}^{(i+1)} = \mathbf{R}^{(i)} + \alpha \mathbf{r}^{(i)}, \quad (1.2)$$

where  $\mathbf{R}^{(i)}$  is the smoothing radius at the  $i$ th iteration,  $\alpha$  is a scalar constant that can be thought of as the step length, and  $\mathbf{r}^{(i)}$  is the residual at the  $i$ th iteration, which can be thought of as the search direction, and is defined as

$$\mathbf{r} = \mathbf{F}[\mathbf{S}_\mathbf{R} \mathbf{d}_h] - \mathbf{F}[\mathbf{d}_l] . \quad (1.3)$$

It can be noted that when equation (1.3) is positive, the higher frequency data still has a higher local frequency value at that specific point than the lower frequency data, thus the higher frequency data is under-smoothed and the smoothing radius should be increased at that point. This follows the form of the first assumption. The second assumption is used when equation (1.3) is negative. When equation (1.3) is zero, the correct radius has been found and no further corrections are made. Thus, it is justifiable to set the search direction from equation (1.2) equal to the residual.

Using the two assumptions, we can continually adjust the smoothing radius until we achieve the desired result of balancing the local frequency content between the two data sets. In practice, this method produces an acceptable solution in approximately 5 iterations and exhibits sublinear convergence. After smoothing the higher

frequency data with the estimated radius, we use the lower frequency and smoothed higher frequency data to estimate time shifts and align the two data sets.

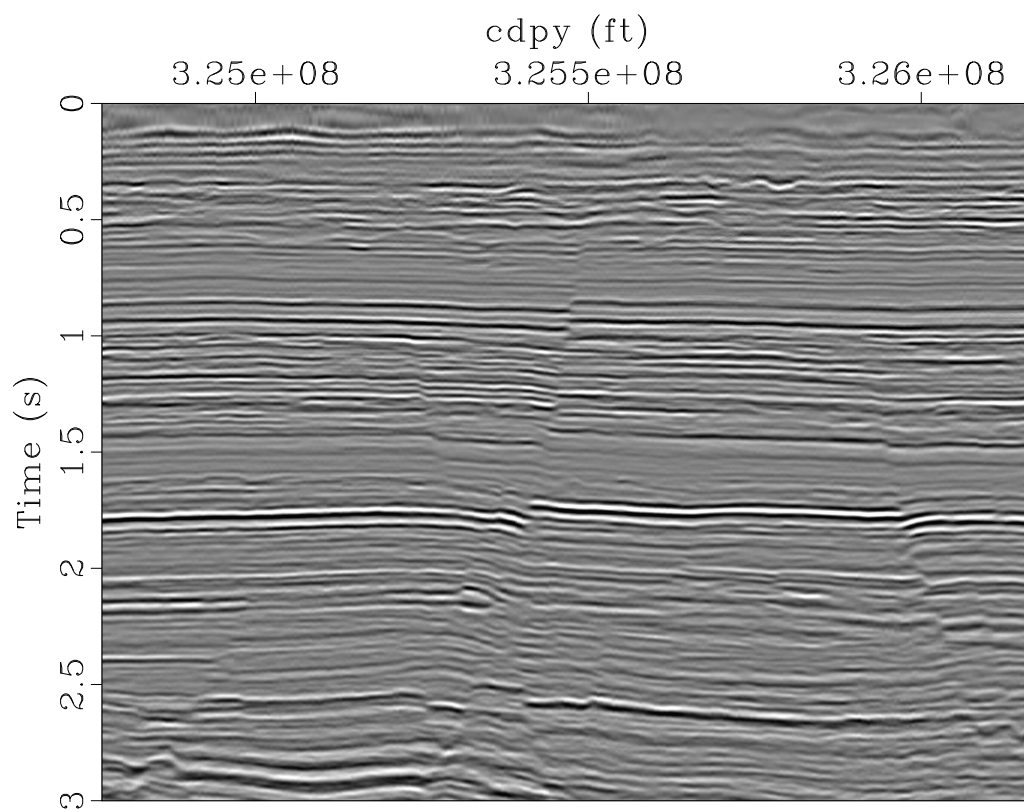
## EXAMPLES

This method is applicable to workflows that require matching data with different frequency content. In this paper, we demonstrate two examples where smoothing data before matching produces better results.

### Matching legacy and high-resolution images

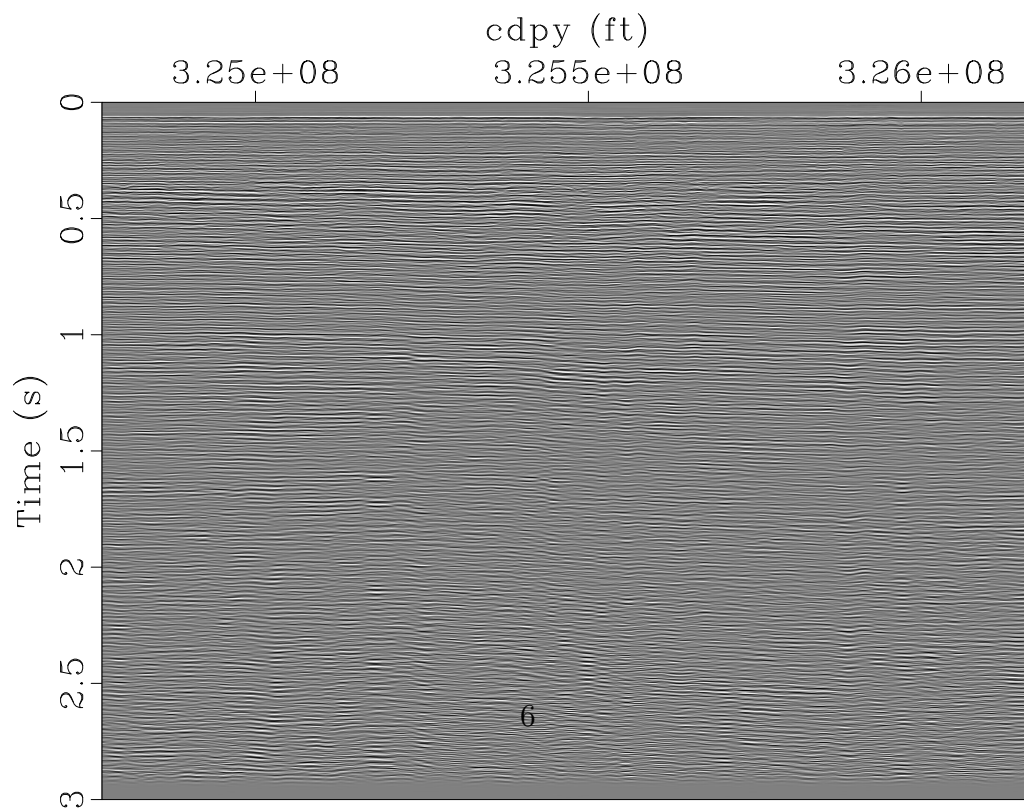
High-resolution seismic data, such as those acquired with the P-cable acquisition system, can produce very detailed images of the near subsurface (Meckel and Mulcahy, 2016). When compared to conventional seismic images, high-resolution images have a higher dominant frequency and a larger frequency bandwidth. However, they usually lack low frequency content and depth coverage that is present in conventional seismic images. As a result, successful interpretation of high-resolution images can be aided by matching with legacy data coverage over the same area.

Example legacy and high-resolution images of the same subsurface are shown in Figure 1.1. The first step in matching the two images is to ensure that they both have a similar frequency bandwidth so they are directly comparable. The average frequency spectra for the two images are shown in Figure 1.3(a). From this, it is evident that there is almost no overlap in frequency bandwidth between the two images. To address this problem, we apply a low-cut filter to the legacy image to remove some of the lower frequencies that are simply not present in the high-resolution image. Next, we implement the method described in the previous section to balance



Legacy

(a)



High-resolution

(b)

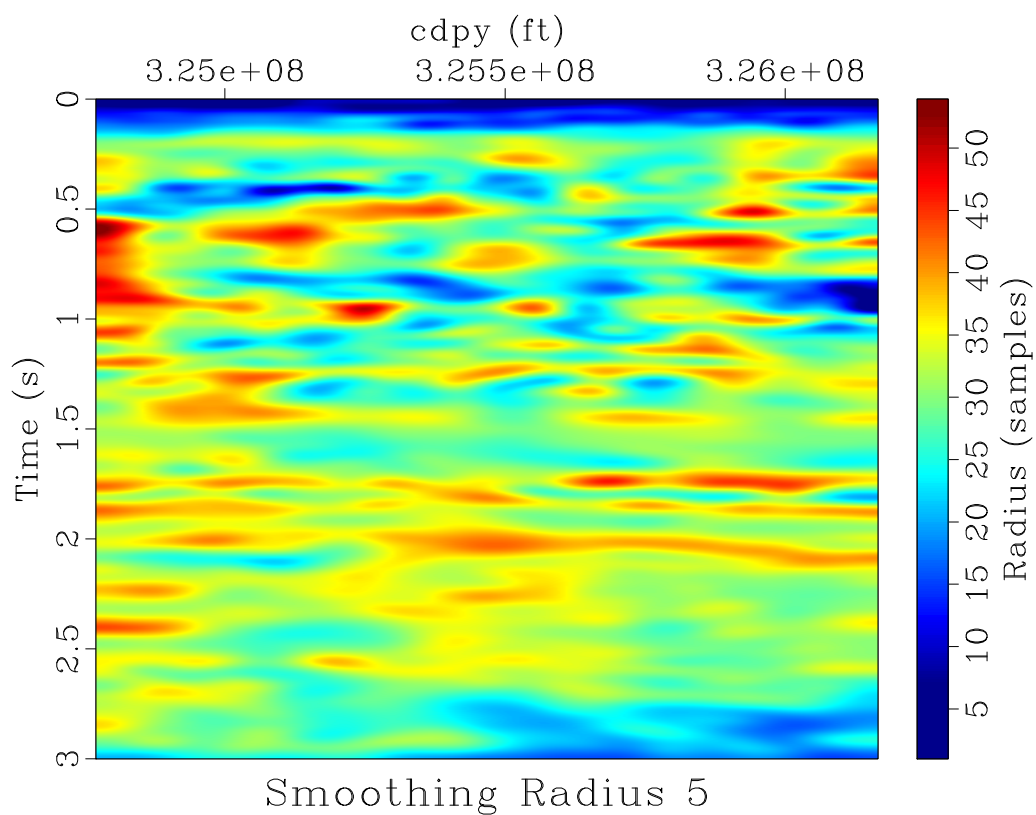


Figure 1.2: The smoothing radius, which is a function of time and space, this method produces after 5 iterations. This represents the number of samples in time that the high-resolution image needs to be smoothed over in a triangle weight to balance local frequency content with the legacy image. chapter-locfreq/merge rect5

local frequency content between the two images. The difference in local frequencies (residual, by equation 1.3) between the high-resolution and legacy images before balancing frequency content and after 5 iterations of the algorithm in equation (1.2) is shown in Figure 1.4. After balancing local frequencies, the images show a similar spectral bandwidth (Figure 1.3(b)), which helps increase the correlation between the two images and makes matching reflections better defined.

After the frequency content is matched, the optimal time shift is found to align signal content between the legacy and high-resolution images. We then apply this time shift to the original high-resolution image—the frequency content is only degraded for the purpose of finding the time shift.

An application of aligning the high-resolution and legacy images is discussed in the companion paper (Greer and Fomel, 2017).

## **Multicomponent image registration**

Multicomponent seismic image registration is an important step before the interpretation of P and S images of the subsurface. It involves warping the space of S images to align reflections with the analogous reflections of P images (Fomel and Backus, 2003; Fomel et al., 2005).

Figure 1.5 shows PP and SS images from a 9-component seismic survey (Fomel, 2007). To properly register the images, we follow the method proposed in Fomel et al. (2005). It consists of three primary steps: (1) initial registration of PP and SS images using initial interpretation and well-log analysis; (2) balancing frequency and amplitude content; and (3) final registration using residual local similarity scanning. We incorporate our method of balancing frequency content into the second step in



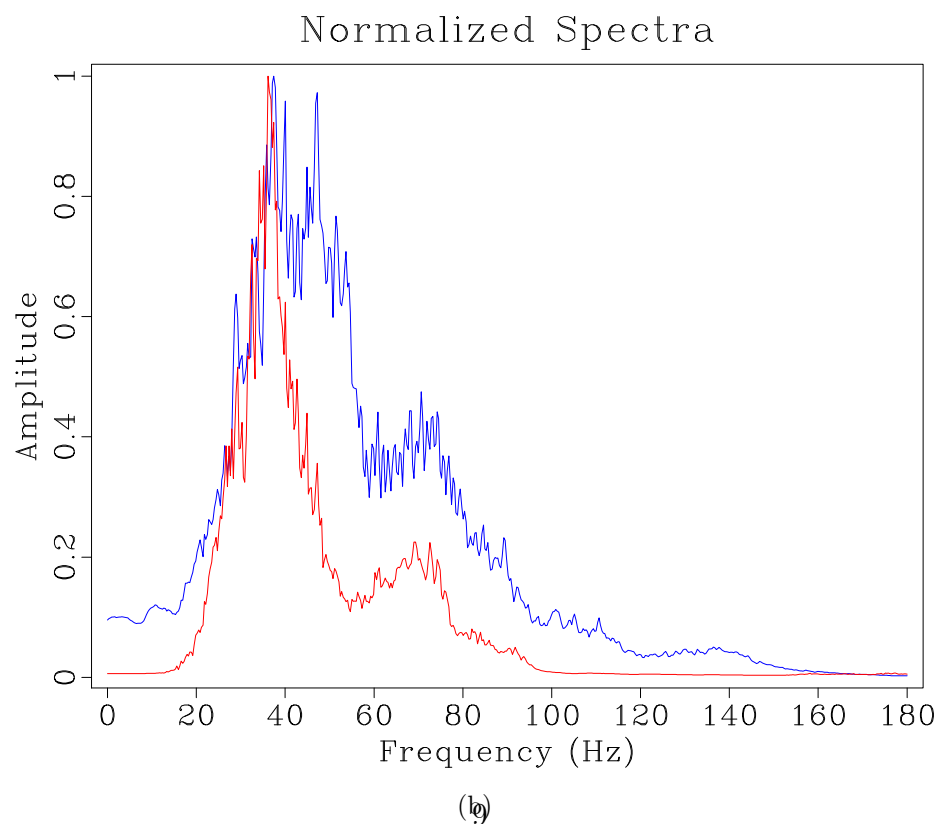
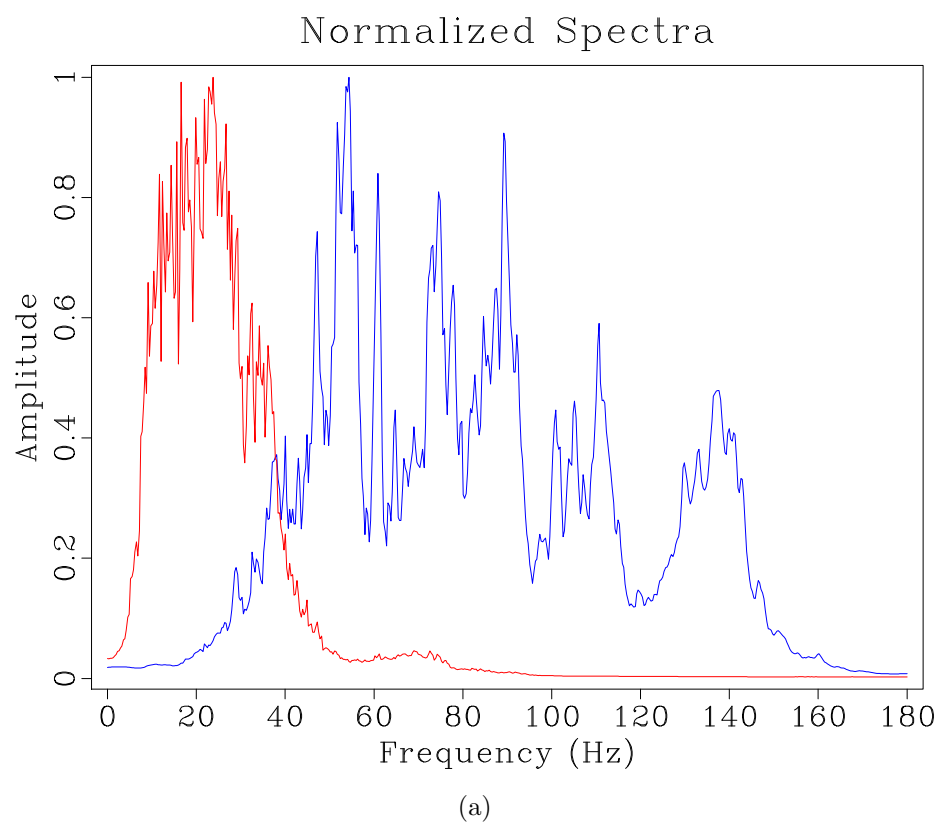


Figure 1.3: Spectral content of the legacy (red) and high-resolution (blue) images before (a) and after (b) spectral balancing.

chapter-locfreq/merge nspectra-orig,high-smooth-spec5

this process.

Before initial registration, the PP image has much higher frequency content than the SS image. After the SS image is temporally compressed to PP time for initial registration, the two images have more similar frequency content. However, additional frequency balancing is still needed before residual registration. This poses a problem as neither image has distinctly higher frequencies than the other, so both images need to be smoothed in different areas to balance frequency content. In order to do this, we modify the proposed method to include two separate smoothing operators—one for each image.

We modify the objective in equation (1.1) as

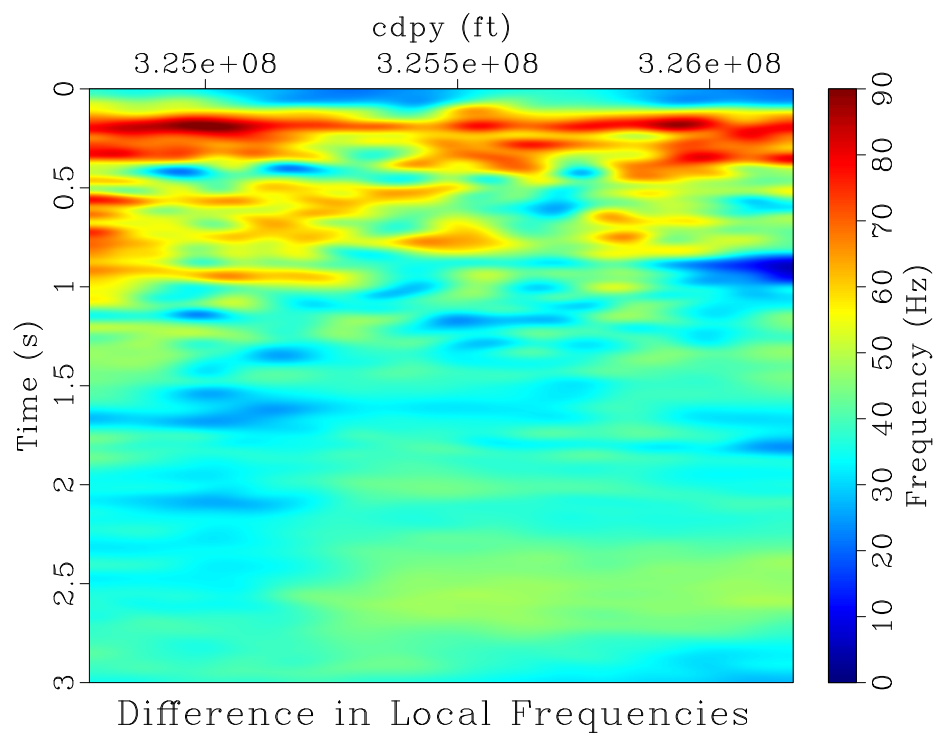
$$\min_{\mathbf{R} \in [-N, -1] \cup [1, N]} \left\| \mathbf{F}[\mathbf{S}_{\mathbf{R}_p} \mathbf{d}_p] - \mathbf{F}[\mathbf{S}_{\mathbf{R}_s} \mathbf{d}_s] \right\|, \quad (1.4)$$

where  $\mathbf{d}_p$  and  $\mathbf{d}_s$  are the PP and SS images, respectively, and  $\mathbf{S}_{\mathbf{R}_p}$  and  $\mathbf{S}_{\mathbf{R}_s}$  are the non-stationary smoothing operators for the PP and SS images, respectively. We also modify the residual from equation (1.3) as

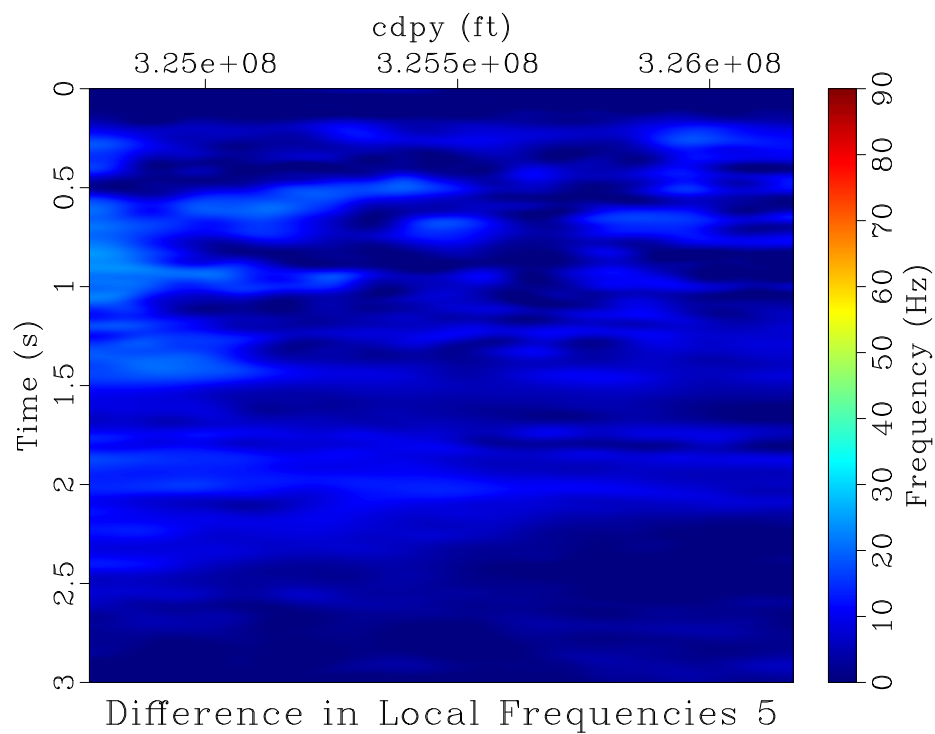
$$\mathbf{r} = \mathbf{F}[\mathbf{S}_{\mathbf{R}_p} \mathbf{d}_p] - \mathbf{F}[\mathbf{S}_{\mathbf{R}_s} \mathbf{d}_s]. \quad (1.5)$$

The ideal radius is still found using the same line-search from equation (1.2), except we allow the smoothing radius to be negative. Physically, a negative smoothing radius would signify that the image should be sharpened at that particular point instead of smoothed. In this case, instead of trying to sharpen the PP image at that particular point, we choose to smooth the SS image by the negative part of the smoothing radius. Thus, we define the  $i$ th components of  $\mathbf{R}_p$  and  $\mathbf{R}_s$  as

$$R_{p,i} = \begin{cases} R_i & \text{if } R_i \geq 1 \\ 1 & \text{otherwise} \end{cases} \quad (1.6)$$



(a)



(b)

Figure 1.4: Difference in local frequencies (residual) between the legacy and high-resolution images before (a) and after (b) the 5th iteration of frequency balancing.

chapter-locfreq/merge freqdif,freqdif-filt5

and

$$R_{s,i} = \begin{cases} |R_i| & \text{if } R_i \leq -1 \\ 1 & \text{otherwise} \end{cases} \quad (1.7)$$

where  $R_i$  is the  $i$ th component of  $\mathbf{R}$  and a radius of 1 represents no smoothing. This allows each image to be smoothed in different areas to balance the frequency content between the two images.

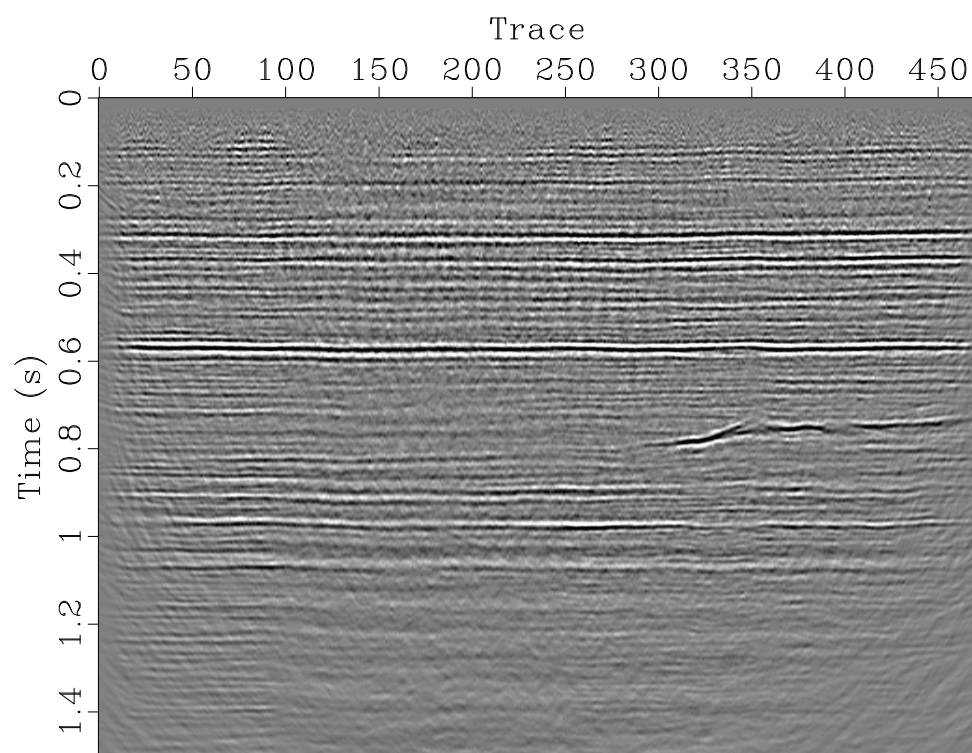
The results of using this spectral balancing method are shown in Figure 1.6. Comparable results were achieved in Liu and Fomel (2012), who used LTFD to balance the spectral content between the two images. However, the method we propose in this paper is more straightforward and significantly less computationally expensive.

## CONCLUSIONS

It is difficult to compare signals with differing frequency content because signals with differing frequencies are hard to correlate. In this paper, we proposed a method of balancing frequency content between data which takes the form of an optimization problem solved by a simple iterative algorithm. It is a relatively inexpensive and effective method compared to previously proposed methods of balancing frequencies between data sets. We applied this method to examples of matching seismic images of differing resolution and for multicomponent image registration.

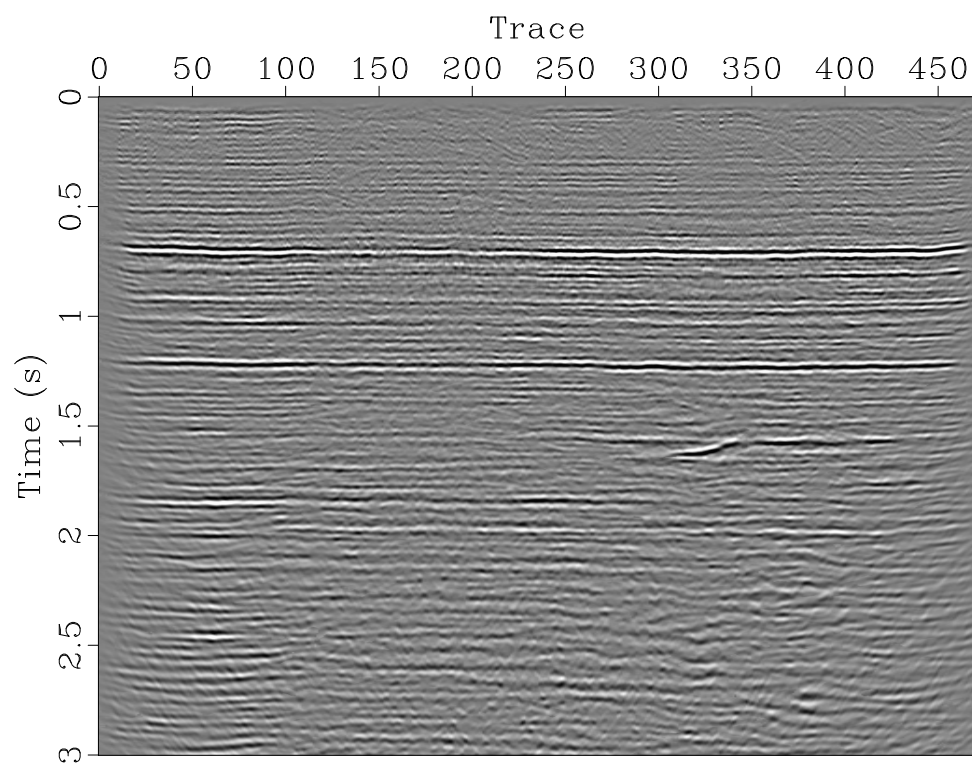
## ACKNOWLEDGEMENTS

We thank the sponsors of the Texas Consortium for Computational Seismology (TCCS) for their financial support.



PP

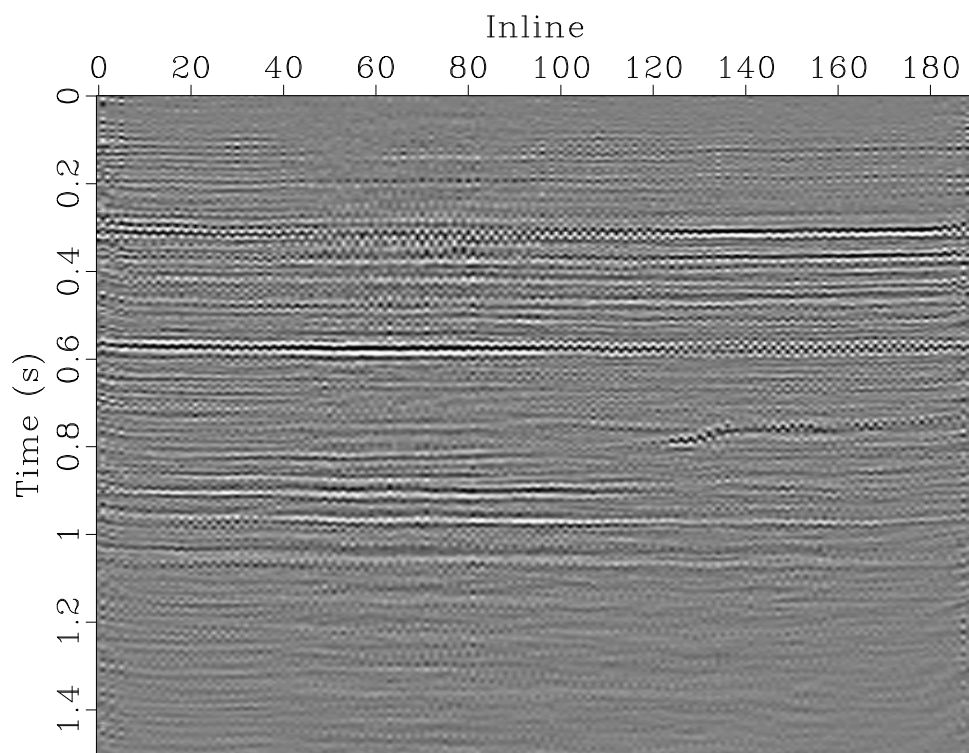
(a)



<sup>13</sup>SS

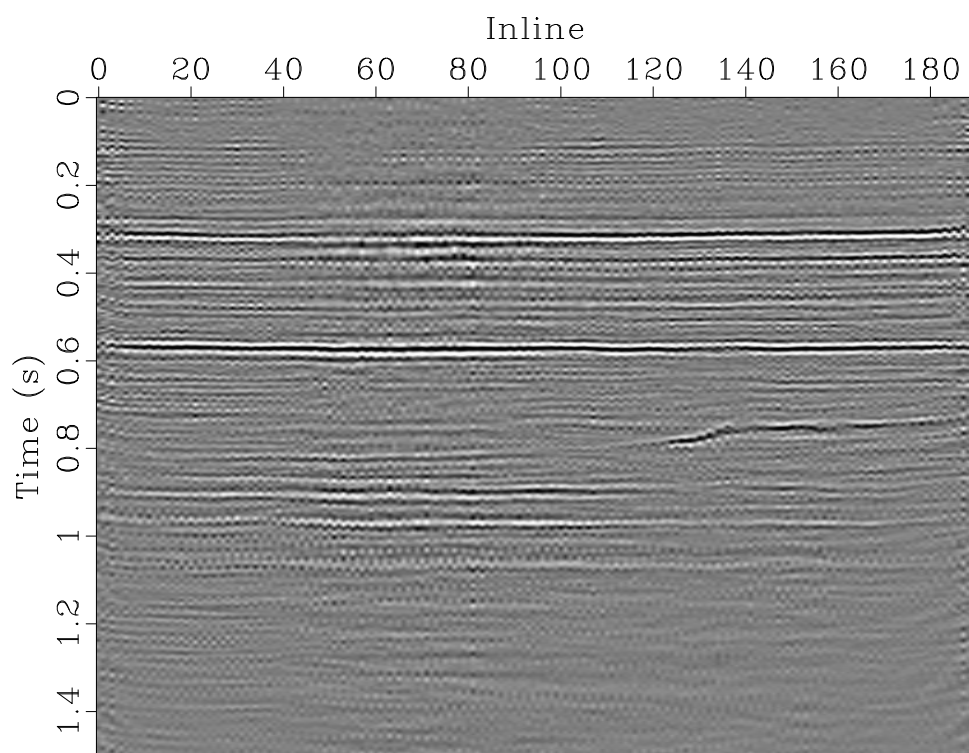
(b)

Figure 1.5: Initial PP (a) and SS (b) images. chapter-locfreq/vecta pp,ss



Interleaved (Before)

(a)



Interleaved (After)

(b)

Figure 1.6: Interleaved PP and warped SS traces before (a) and after (b) frequency balancing and residual registration. After registration, the signal content between the two initial images is more aligned: for example, the reflections around 0.3 and 0.6 s.

## Bibliography

- Fomel, S., 2007, Local seismic attributes: *Geophysics*, **72**, A29–A33.
- Fomel, S., M. Backus, K. Fouad, B. Hardage, and G. Winters, 2005, A multistep approach to multicomponent seismic image registration with application to a West Texas carbonate reservoir study: 75th Ann. Internat. Mtg, Soc. of Expl. Geophys., 1018–1021.
- Fomel, S., and M. M. Backus, 2003, Multicomponent seismic data registration by least squares: 73rd Annual International Meeting, Soc. of Expl. Geophys., 701–784.
- Fomel, S., and L. Jin, 2009, Time-lapse image registration using the local similarity attribute: *Geophysics*, **74**, A7–A11.
- Greer, S., and S. Fomel, 2017, Matching and merging high resolution and legacy seismic images: Presented at the 87th Annual International Meeting, Society of Exploration Geophysicists. (Submitted).
- Hale, D., 2013, Dynamic warping of seismic images: *GEOPHYSICS*, **78**, S105–S115.
- Herrera, R. H., S. Fomel, and M. van der Baan, 2014, Automatic approaches for seismic to well tying: *Interpretation*, **2**, SD9–SD17.
- Herrera, R. H., and M. van der Baan, 2012, Guided seismic-to-well tying based on dynamic time warping: 82nd Annual International Meeting, Society of Exploration Geophysicists, 1–5.
- Liu, Y., and S. Fomel, 2012, Seismic data analysis using local time-frequency decomposition: *Geophysical Prospecting*, **61**, 516–525.
- Lumley, D., D. C. Adams, M. Meadows, S. Cole, and R. Wright, 2003, 4D seismic

data processing issues and examples: 73rd Annual International Meeting, Society of Exploration Geophysicists, 1394–1397.

Meckel, T. A., and F. J. Mulcahy, 2016, Use of novel high-resolution 3D marine seismic technology to evaluate Quaternary fluvial valley development and geologic controls on shallow gas distribution, inner shelf, Gulf of Mexico: Interpretation, **4**, SC35–SC49.

Ursenbach, C., P. Cary, and M. Perz, 2013, Limits on resolution enhancement for PS data mapped to PP time: The Leading Edge, **32**, 64–71.

White, R. E., 1991, Properties of instantaneous seismic attributes: The Leading Edge, **10**, 26–32.



## Vita

Sarah graduated with high honors from Cinco Ranch High School in Katy, Texas in 2014 and came to The University of Texas at Austin (UT Austin) to pursue her undergraduate studies. She is a candidate for two Bachelor of Science degrees from UT Austin in Geological Sciences and Mathematics. After graduation, she plans on pursuing a PhD in Computational and Mathematical Engineering from Stanford University.

Permanent address: 2175 Stonecrest Drive, Eugene, OR, 97401, USA

This thesis was typeset with  $\text{\LaTeX}^\dagger$  by the author.

---

<sup>†</sup> $\text{\LaTeX}$  is a document preparation system developed by Leslie Lamport as a special version of Donald Knuth's  $\text{\TeX}$  Program.